Quark matter under strong magnetic fields in the su(3) Nambu–Jona-Lasinio model

D. P. Menezes,[1] M. Benghi Pinto,[1] S. S. Avancini,[1] and C. Providência[2]

[1]*Depto de Física, CFM, Universidade Federal de Santa Catarina, C.P. 476, CEP 88.040-900, Florianópolis, SC, Brazil*

[2]*Centro de Física Computacional, Department of Physics, University of Coimbra, P-3004-516, Coimbra, Portugal*

(Received 8 July 2009; revised manuscript received 20 October 2009; published 17 December 2009)

In the present work we use the mean-field approximation to investigate quark matter described by the su(3) Nambu–Jona-Lasinio (NJL) model subject to a strong magnetic field. We consider two cases: pure quark matter and quark matter in β equilibrium possibly present in magnetars. The results are compared with the ones obtained with the su(2) version of the model. The energy per baryon of magnetized quark matter becomes more bound than nuclear matter made of iron nuclei, for B around 2×10^{19} G. When the su(3) NJL model is applied to stellar matter, the maximum mass configurations are always above $1.45 M_\odot$ and may be as high as $1.86 M_\odot$ for a central magnetic field of 5×10^{18} G. These numbers are within the masses of observed neutron stars.

DOI: 10.1103/PhysRevC.80.065805 PACS number(s): 26.60.−c, 11.10.−z, 21.65.Qr, 24.10.Jv

I. INTRODUCTION

In noncentral heavy-ion collisions such as the ones performed at the BNL Relativistic Heavy Ion Collider (RHIC) and the CERN Large Hadron Collider (LHC), physicists have been looking for a possible signature of the presence of charge parity (CP)-odd domains in the presumably formed quark-gluon plasma phase [1]. The study of deconfined quark matter subject to strong external magnetic fields is then mandatory if one intends to understand the physics taking place in such colliders.

Neutron stars with very strong magnetic fields of the order of 10^{14}–10^{15} G are known as magnetars and they are believed to be the sources of the intense γ and x rays detected in 1979 [2,3]. The hypothesis that some neutron stars are constituted by unbound quark matter cannot be completely ruled out [4] because the Bodmer-Witten conjecture [5] cannot be tested on earthly experiments. This conjecture implies that the true ground state of all matter is (unbound) quark matter because theoretical predictions show that its energy per baryon at zero pressure is lower than ^{56}Fe binding energy.

In the present work our aim is to investigate quark matter described by the su(3) version of the Nambu-Jona-Lasinio (NJL) [6] model exposed to strong magnetic fields. In the case of pure quark matter, as predicted by the QCD phase transition possibly taking place in heavy-ion collisions, the magnetic field is certainly external. In the case of neutron stars, the magnetic field can be generated by the alignment of charged particles that are spinning very rapidly. We next use an external field to mimic the real situation, which we do not know how to determine. Albeit in an approximate way, the effect of the magnetic field on the macroscopic quantities such as radius and mass can be obtained.

Recently the su(2) version of the NJL model was used to treat both situations described previously [7]. We have shown that, for pure quark matter, the energy per baryon for magnetized quark matter has a minimum that is lower than the one determined for magnetic free quark matter. We have also determined that a magnetic field of the order of 2×10^{18} G barely affects the effective mass as compared with the results for matter not subject to the magnetic field. For $B = 5 \times 10^{19}$ G, matter is totally polarized for chemical potentials below 490 MeV. For small values of the magnetic fields the number of filled Landau levels (LL) is large and the quantization effects are washed out, whereas for large magnetic fields the chiral symmetry restoration occurs for smaller values of the chemical potentials. When β equilibrium is enforced, the numerical results show that, for the the su(2) case, only very high magnetic fields ($B \geqslant 10^{18}$ G) affect the equation of state (EOS) in a noticeable way.

The NJL su(3) model has been discussed in many articles [8–10]. In the present article we adopt the parametrization proposed in Ref. [9], which has been chosen so that the vacuum properties of the pion, kaon, and η are reproduced, and study the properties of the quark stars predicted by this model in the presence of a magnetic field. The inclusion of the s quarks, necessary in the su(3) NJL model, poses some new numerical difficulties and some questions that need to be addressed. Those problems are tackled throughout the article. One of the questions was raised in Refs. [11,12] and refers to the stability of quark matter described by the NJL model. The authors show that it is not absolutely stable. As already mentioned, in Ref. [7] we have seen that the inclusion of the magnetic field increases stability in the su(2) version and the same behavior is expected in the su(3) NJL, which is shown next.

This article is organized is such a way that all calculations already shown explicitly in Ref. [7] are not repeated but all important differences are outlined. In Secs. II and III the formalism (mean-field theory) and the equations of state are shown and in Sec. IV the final results are displayed and the conclusions are drawn.

II. GENERAL FORMALISM

To consider (three flavor) quark stars in β equilibrium with strong magnetic fields we introduce the following Lagrangian density,

$$\mathcal{L} = \mathcal{L}_f + \mathcal{L}_l - \frac{1}{4} F_{\mu\nu} F^{\mu\nu}, \tag{1}$$

where the quark sector is described by the su(3) version of the NJL model [8], which includes a scalar-pseudoscalar interaction and the t'Hooft six-fermion interaction, that models the axial $U(1)_A$ symmetry breaking:

$$\mathcal{L}_f = \bar{\psi}_f[\gamma_\mu(i\partial^\mu - q_f A^\mu) - \hat{m}_c]\psi_f + \mathcal{L}_{\rm sym} + \mathcal{L}_{\rm det}, \tag{2}$$

where $\mathcal{L}_{\rm sym}$ and $\mathcal{L}_{\rm det}$ are given by

$$\mathcal{L}_{\rm sym} = G\sum_{a=0}^{8}[(\bar{\psi}_f\lambda_a\psi_f)^2 + (\bar{\psi}_f i\gamma_5\lambda_a\psi_f)^2], \tag{3}$$

$$\mathcal{L}_{\rm det} = -K\{\det{}_f[\bar{\psi}_f(1+\gamma_5)\psi_f] + \det{}_f[\bar{\psi}_f(1-\gamma_5)\psi_f]\}, \tag{4}$$

where $\psi_f = (u, d, s)^T$ represents a quark field with three flavors, $\hat{m}_c = \mathrm{diag}_f(m_u, m_d, m_s)$ is the corresponding (current) mass matrix while q_f represents the quark electric charge; $\lambda_0 = \sqrt{2/3}I$, where I is the unit matrix in the three flavor space; and $0 < \lambda_a \leqslant 8$ denote the Gell-Mann matrices. Here, we consider $m_u = m_d \neq m_s$. The $\mathcal{L}_{\rm det}$ term is the t'Hooft interaction that represents a determinant in flavor space, which, for three flavor, gives a six-point interaction [10] and is essential in the calculation of the mass splitting of the η mesons

$$\det{}_f(\bar{\psi}_f\mathcal{O}\psi_f) := \sum_{i,j,k}\epsilon_{ijk}(\bar{u}\mathcal{O}\psi_i)(\bar{d}\mathcal{O}\psi_j)(\bar{s}\mathcal{O}\psi_k), \tag{5}$$

where ϵ_{ijk} is the usual three-dimensional Levi-Civita symbol. The Lagrangian also contains the $\mathcal{L}_{\rm sym}$ term, which is symmetric under global $U(N_f)_L \times U(N_f)_R$ transformations and corresponds to a four-point interaction in flavor space. In the Appendix we discuss the steps to obtain $\mathcal{L}_f$ in the mean-field approximation (MFA). The model is not renormalizable, and as a regularization scheme for the divergent ultraviolet integrals we use a sharp cutoff Λ in the three-momentum space. The parameters of the model, Λ, the coupling constants G and K, and the current quark masses m_u^0 and m_s^0 are determined by fitting f_π, m_π, m_K, and $m_{\eta'}$ to their empirical values.

The leptonic sector is given by

$$\mathcal{L}_l = \bar{\psi}_l[\gamma_\mu(i\partial^\mu - q_l A^\mu) - m_l]\psi_l, \tag{6}$$

where $l = e, \mu$. One recognizes this sector as being represented by the usual QED type of Lagrangian density. As usual, A_μ and $F_{\mu\nu} = \partial_\mu A_\nu - \partial_\nu A_\mu$ are used to account for the external magnetic field. Then, because we are interested in a static and constant magnetic field in the z direction, $A_\mu = \delta_{\mu 2}x_1 B$.

III. THE EOS

We need to evaluate the thermodynamical potential for the three-flavor quark sector, Ω_f, which as usual can be written as $\Omega_f = -P_f = \mathcal{E}_f - T\mathcal{S} - \sum_f \mu_f\rho_f$, where P_f represents the pressure, $\mathcal{E}_f$ the energy density, T the temperature, $\mathcal{S}$ the entropy density, and μ_f the chemical potential.

For the present study, just the zero temperature case is important and, as a consequence, the term with the entropy vanishes. The total pressure for three flavor quark matter in β equilibrium is given by

$$P(\mu_f, \mu_l, B) = P_f^N\big|_{M_f} + P_l^N\big|_{m_l} + \frac{B^2}{2}, \tag{7}$$

where our notation means that P_f^N is evaluated in terms of the quark effective mass, M_f, which is determined in a (nonperturbative) self-consistent way while P_l^N is evaluated at the leptonic bare mass, m_l. The term $B^2/2$ arises due to the electromagnetic term $F_{\mu\nu}F^{\mu\nu}/4$ in the original Lagrangian density. The subscript N indicates normalized pressures. Here, our normalization choice is such that $P_f^N = 0$ at $\mu_f = 0$ ($f = u, s, d$) and $P_l^N = 0$ at $\mu_l = 0$ ($l = e, \mu$), implying that $P(0, 0, B) = B^2/2$. This choice of renormalization was done because we want to study the structure of neutron stars under the influence of strong magnetic fields. To obtain the total energy density and pressure relevant for neutron star structure, the contribution from the electromagnetic field must be included.

A. Quark contribution to the EOS

In the mean-field approximation the pressure can be written as

$$P_f = \theta_u + \theta_d + \theta_s - 2G\left(\phi_u^2 + \phi_d^2 + \phi_s^2\right) + 4K\phi_u\phi_d\phi_s, \tag{8}$$

where an irrelevant term has been discarded. The pressure due to the three quarks is diagrammatically represented in Fig. 1(a).

For a given flavor, the θ_f term is given by

$$\theta_f = -\frac{i}{2}\mathrm{tr}\int\frac{d^4p}{(2\pi)^4}\ln\left(-p^2 + M_f^2\right) \tag{9}$$

and the condensates ϕ_f are given by

$$\phi_f = \langle\bar{\psi}_f\psi_f\rangle = -i\int\frac{d^4p}{(2\pi)^4}\mathrm{tr}\frac{1}{(\not{p} - M_f + i\epsilon)}, \tag{10}$$

where, according to standard Feynman rules for this model, all the traces are to be taken over color ($N_c = 3$) and Dirac

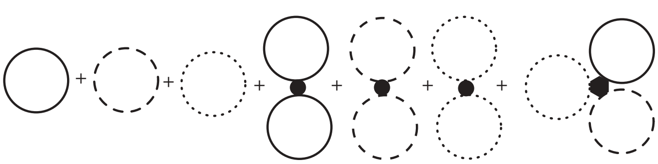

(a)

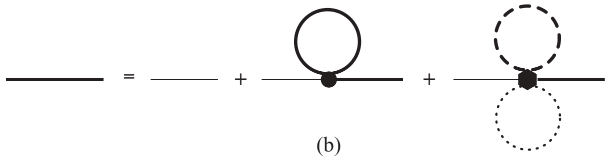

(b)

FIG. 1. (a) Feynman diagrams contributing to the quark pressure in the MFA. The lines represent the three dressed quark propagators for the different flavors: u (continuous line), d (dashed line), and s (dotted line). The black dot represents G and the black hexagon represents K. (b) Diagrammatic representation of the effective mass for flavor u. The diagrams contributing to the other two flavors display the same topology.

space, but not flavor. Also, a minus sign that accounts for antisymmetry has been included so that, for a given flavor, each quark loop generates an overall $-4N_c$ factor. To obtain results valid at finite T and μ in the presence of an external magnetic field B one can use the following replacements [13]:

$$p_0 \to i(\omega_\nu - i\mu_f),$$
$$\mathbf{p}^2 \to p_z^2 + (2n+1-s), \quad \text{with } s = \pm 1,\ n = 0, 1, \ldots$$
$$\int \frac{d^4p}{(2\pi)^4} \to i\frac{T|q_f|B}{2\pi} \sum_{\nu=-\infty}^{\infty} \sum_{n=0}^{\infty} \int \frac{dp_z}{(2\pi)}.$$

In the above relations, $\omega_\nu = (2\nu+1)\pi T$, with $\nu = 0, \pm 1, \pm 2, \ldots$ representing the Matsubara frequencies for fermions while n represents the Landau levels (LL) and s represents the spin states, which, at $B \neq 0$, must be treated separately. The case $T = 0$ in which we are interested can be easily obtained after the aforementioned substitutions (see Ref. [7]).

The effective quark masses can be obtained self consistently from [see Fig. 1(b)]

$$M_i = m_i - 4G\phi_i + 2K\phi_j\phi_k, \tag{11}$$

with (i, j, k) being any permutation of (u, d, s). So, to determine the EOS for the su(3) NJL at finite density and in the presence of a magnetic field we need to know the condensates, ϕ_f, as well as the contribution from the gas of quasiparticles, θ_f. Both quantities, which are related by $\phi_f \sim d\theta_f/dM_f$, have been evaluated with great detail in Ref. [7]. Here, we just quote the results

$$P_f = \left(P_f^{\rm vac} + P_f^{\rm mag} + P_f^{\rm med}\right)_{M_f}, \tag{12}$$

where the vacuum contribution reads

$$P_f^{\rm vac} = -\frac{N_c}{8\pi^2}\left\{M_f^4 \ln\left[\frac{(\Lambda+\epsilon_\Lambda)}{M_f}\right] - \epsilon_\Lambda\, \Lambda\left(\Lambda^2 + \epsilon_\Lambda^2\right)\right\}, \tag{13}$$

where we have defined $\epsilon_\Lambda = \sqrt{\Lambda^2 + M_f^2}$ with Λ representing a non-covariant ultraviolet cutoff. The evaluations performed in Ref. [7] also give the following finite magnetic contribution

$$P_f^{\rm mag} = \frac{N_c(|q_f|B)^2}{2\pi^2}\left[\zeta'(-1, x_f) - \frac{1}{2}\left(x_f^2 - x_f\right)\ln x_f + \frac{x_f^2}{4}\right], \tag{14}$$

where $x_f = M_f^2/(2|q_f|B)$ while $\zeta'(-1, x_f) = d\zeta(z, x_f)/dz|_{z=-1}$, where $\zeta(z, x_f)$ is the Riemann-Hurwitz ζ function [14]. Finally, after integration, the medium contribution can be written as

$$P_{M_f}^{\rm med} = \sum_{k=0}^{k_{f,\max}} \alpha_k \frac{|q_f|BN_c}{4\pi^2}\left[\mu_f\sqrt{\mu_f^2 - s_f(k,B)^2} - s_f(k,B)^2 \ln\left(\frac{\mu_f + \sqrt{\mu_f^2 - s_f(k,B)^2}}{s_f(k,B)}\right)\right], \tag{15}$$

where $s_f(k, B) = \sqrt{M_f^2 + 2|q_f|Bk}$, $\alpha_0 = 1$, and $\alpha_{k>0} = 2$. The upper Landau level (or the nearest integer) is defined by

$$k_{f,\max} = \frac{\mu_f^2 - M_f^2}{2|q_f|B} = \frac{p_{f,F}^2}{2|q_f|B}. \tag{16}$$

Finally, the condensates ϕ_f entering the quark pressure at finite density and in the presence of an external magnetic field can also be written as

$$\phi_f = \left(\phi_f^{\rm vac} + \phi_f^{\rm mag} + \phi_f^{\rm med}\right)_{M_f}, \tag{17}$$

where

$$\phi_f^{\rm vac} = -\frac{M_f N_c}{2\pi^2}\left[\Lambda\epsilon_\Lambda - M_f^2 \ln\left(\frac{\Lambda+\epsilon_\Lambda}{M_f}\right)\right], \tag{18}$$

$$\phi_f^{\rm mag} = -\frac{M_f|q_f|BN_c}{2\pi^2}\left[\ln\Gamma(x_f) - \frac{1}{2}\ln(2\pi) + x_f - \frac{1}{2}(2x_f - 1)\ln(x_f)\right], \tag{19}$$

and

$$\phi_f^{\rm med} = \sum_{k=0}^{k_{f,\max}} \alpha_k \frac{M_f|q_f|BN_c}{2\pi^2} \times \left[\ln\left(\frac{\mu_f + \sqrt{\mu_f^2 - s_f(k,B)^2}}{s_f(k,B)}\right)\right]. \tag{20}$$

From the pressure one can obtain the density, ρ_f, corresponding to each different flavor, which is given by

$$\rho_f = \sum_{k=0}^{k_{f,\max}} \alpha_k \frac{|q_f|BN_c}{2\pi^2} k_{F,f}, \tag{21}$$

where $k_{F,f} = \sqrt{\mu_f^2 - s_f(k,B)^2}$, because $dP/d\phi_f = 0$.

The quark contribution to the energy density is

$$\mathcal{E}_f(\mu_f, B) = -P_f^N + \sum_f \mu_f\rho_f, \tag{22}$$

where $P_f^N = P_f(\mu_f)|_{M_f(\mu_f)} - P_f(0)|_{M_f(0)}$.

Throughout this article we consider the following set of parameters [9]: $\Lambda = 631.4$ MeV, $m_u = m_d = 5.5$ MeV, $m_s = 135.7$ MeV, $G\Lambda^2 = 1.835$, and $K\Lambda^5 = 9.29$.

B. Lepton contribution to the EOS

The leptonic contribution, P_l, has also been evaluated in detail in Ref. [7] where the normalization requirement $P_l^N = 0$ at $\mu_l = 0$ has been adopted. The result shows that, at the one loop level, only the following (finite) medium contribution must be considered:

$$P_l^N = \sum_{l=e}^{\mu} \sum_{k=0}^{k_{l,\max}} \alpha_k \frac{|q_l|B}{4\pi^2}\left[\mu_l\sqrt{\mu_l^2 - s_l(k,B)^2} - s_l(k,B)^2 \ln\left(\frac{\mu_l + \sqrt{\mu_l^2 - s_l(k,B)^2}}{s_l(k,B)}\right)\right]. \tag{23}$$

Then, the leptonic density is also easily evaluated yielding

$$\rho_l = \sum_{k=0}^{k_{l,\max}} \alpha_k \frac{|q_l|B}{2\pi^2} k_{F,l}(k, s_l), \tag{24}$$

where $k_{F,l}(k, s_l) = \sqrt{\mu_l^2 - s_l(k, B)^2}$. Finally, the leptonic energy density reads

$$\mathcal{E}_l(\mu_l, B) = -P_l^N + \sum_l \mu_l \rho_l. \tag{25}$$

The lepton masses are $m_e = 0.511$ MeV and $m_\mu = 105.66$ MeV. We have not considered the effect of the magnetic field on the mass of the electron, because, as discussed in Ref. [15] and later in Refs. [16,17], although the electron mass grows heavier than m_e for $B > 0.65 B_e$, with $B_e = 4.4 \times 10^{13}$ G, it needs a field as strong as 10^{32} G to have its ground state energy doubled [17]. For 10^{18} G the effective mass of the electron just exceeds m_e by approximately 8%. Taking into account that in β-equilibrium quark matter in compact stars the fraction of electron does not exceed 1.5%, a different electron mass would not affect the results even if we had taken a value twice as large for the mass of the electron (i.e., 2 m_e).

IV. RESULTS AND CONCLUSIONS

In the sequel we consider two different situations of quark matter under a strong magnetic field: (a) pure quark matter with the same chemical potential for all quark flavors, and (b) β-equilibrium quark stellar matter.

We first discuss the properties of pure quark matter with equal chemical potentials for all flavors, namely, the behavior of the dynamical quark masses, the chiral symmetry restoration with density, and the energy per baryon. In Fig. 2 we display the masses of quarks u and d as a function of the chemical potential for different values of the magnetic field and the two versions of the NJL model. For the magnetic field intensities used, one can clearly identify the filling of different Landau levels causing the usual kinks in the curves. For the three intensities considered the chiral symmetry is approximately restored for $\mu = 400$ MeV.

It is interesting to see that although the general behavior is the same, the effect of the LL is more pronounced in the su(2) version.

In Fig. 3 the mass of the s quark is shown as a function of the chemical potential for different values of the magnetic field. One can see how drastically it falls around $\mu = 450$ MeV. For magnetic free quark matter, this is the same behavior shown in Fig. 3 of Ref. [18]. One can observe that the curve is no longer smooth when B is turned on, but the values of the strange quark mass do not vary much. According to Ref. [18], the fact that the strange quark mass remains relatively high as compared with the masses of the other two quarks is the main reason why deconfined quark matter may not be likely to appear in the core of hybrid neutron stars. For a magnetic field larger than 10^{19} the restoration of chiral symmetry for the s quark occurs in steps and starts at a smaller chemical potential than in the $B = 0$ case.

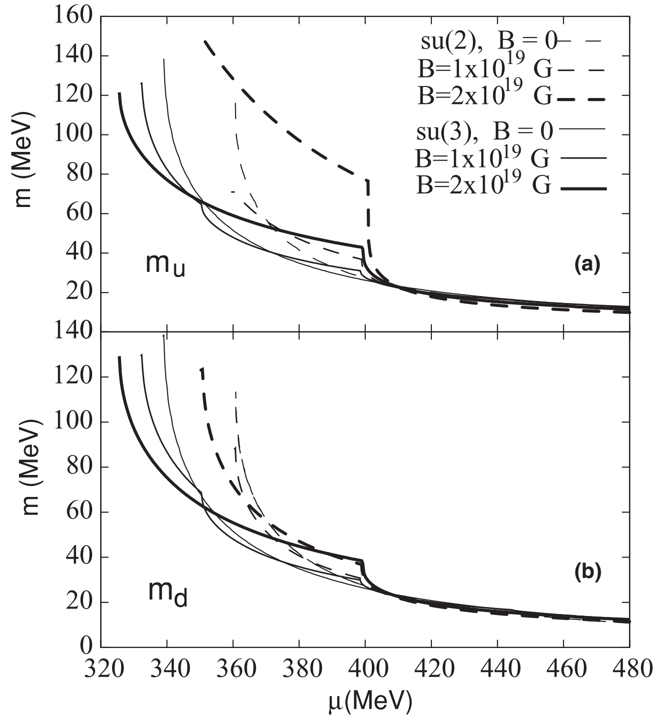

FIG. 2. Mass of the quarks (a) u and (b) d as a function of the chemical potential for $B = 0$, 10^{19}, and 2×10^{19} G within the su(2) NJL and the su(3) NJL.

The phenomenon of magnetic catalysis, which enhances chiral symmetry breaking, has been well discussed within the su(2) version of the NJL model [19]. Here, for reference, we show the vacuum effective mass of the three quarks as a function of the magnetic field in Fig. 4. For $B > 10^{19}$ G the vacuum masses increase dramatically with the magnetic field as expected. A similar increase of the vacuum mass was also obtained for the su(2) version of NJL in Refs. [7,19] and the effect is related to the fact that the B field facilitates the binding by antialigning the helicities of the quark and the antiquark, which are then bound by the NJL interaction. As shown in Fig. 4, an

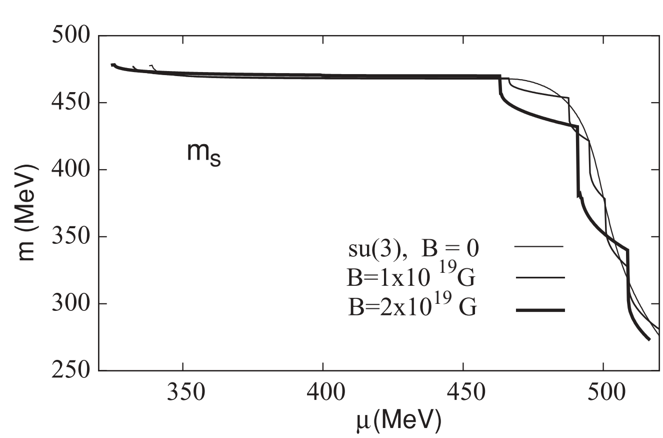

FIG. 3. Mass of the s quarks as a function of the chemical potential for $B = 0$, 10^{19}, and 2×10^{19} G within su(3) NJL.

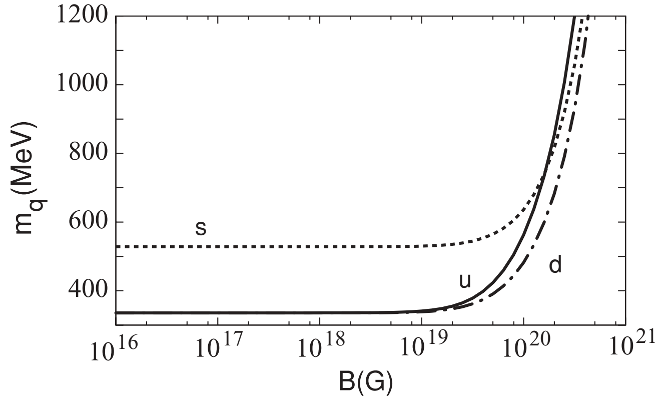

FIG. 4. Vacuum mass of the quarks as a function of the magnetic field B.

interesting result of the su(3) version is that, because of its larger electric charge, the u quark has an effective mass that becomes larger than that of the s quark for $B > 1.5 \times 10^{20}$ G.

The same phenomenon of magnetic catalysis occurs at finite density: for a given baryonic density the quark effective masses are larger for a larger magnetic field. This may not be obvious from Figs. 2 and 3, where the the effective mass is plotted against the chemical potential and not the baryonic density. We point out that there are two opposite effects that must be considered when discussing the effective mass of quarks: the constituent quark mass increases with the magnetic field and decreases with the density. As seen in Fig. 5, where the baryonic density is shown as a function of the quark chemical potential for two values of the magnetic field and for both versions of the NJL model, su(2) and su(3), the relation between the chemical potential and the baryonic density is not linear.

Let us consider, for instance, the chemical potentials 340 and 360 MeV in Fig. 2. For $\mu = 340$ MeV the largest mass corresponds to the zero field curve and the smallest one to the largest field considered, which seems to be inconsistent with the magnetic field catalysis. However, looking at Fig. 5, it is seen that for $\mu = 340$ MeV the baryonic density is approximately 0.3 fm^{-3} for $B = 0$ G, 0.32 fm^{-3} for $B = 10^{19}$ G, and 0.35 fm^{-3} for $B = 2 \times 10^{19}$ G. This means that the effect

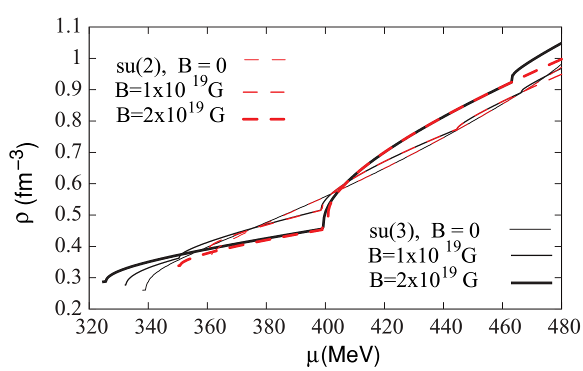

FIG. 5. (Color online) Baryonic density as a function of the quark chemical potential for $B = 0$, 10^{19}, and 2×10^{19} G within both su(2) and su(3) NJL.

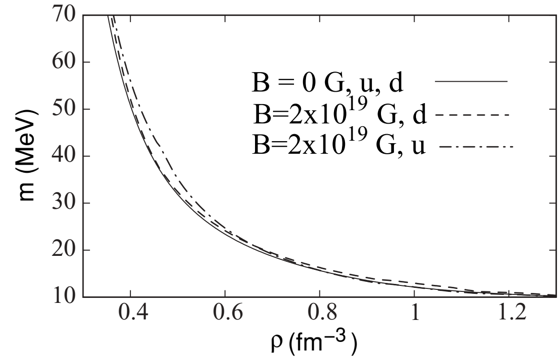

FIG. 6. Mass of the quarks u and d as a function of the baryonic density for $B = 0$ and 2×10^{19} G within su(3) NJL.

of the density is stronger than the effect of the magnetic field and the situation with the largest density ($B = 2 \times 10^{19}$ G) has the smallest mass. Now let us consider $\mu = 360$ MeV. In this case the baryonic densities for $B = 0$ and $B = 2 \times 10^{19}$ G are approximately equal, that is, $\sim$0.39 fm^{-3}, whereas for $B = 10^{19}$ the baryonic density is $\sim$0.41 fm^{-3}. It is seen in Fig. 2 that for $\mu = 360$ MeV the smallest mass corresponds to $B = 10^{19}$ G with the largest baryonic density. However, the largest mass corresponds to $B = 2 \times 10^{19}$ G that, although associated with a density slightly smaller than the one for $B = 0$, has a larger field and, therefore, the magnetic field catalysis is observed. The magnetic catalysis at finite density is clearly seen in Fig. 6 where the masses of quarks u and d are plotted in terms of the baryonic density for $B = 0$ and 2×10^{19} G.

As already noticed in Ref. [7], for small values of the magnetic fields the number of filled LL is quite large and the effects of the quantization are less visible. Because of the Landau quantization, the increase of the strength of the magnetic field gives rise to a decrease of the number of the filled LL and the amplitude of the oscillations is more clear in the graphics. For each value of the magnetic field, the kink appearing at the smallest chemical potential in Fig. 5 corresponds to the case where only the first LL has been occupied.

In Fig. 7 one can see that the inclusion of the magnetic field makes matter more and more bound in both versions of the model. For the present set of parameters, the energy per baryon E/A of magnetized quark matter becomes more bound than nuclear matter made of iron nuclei, $\frac{E}{A}|_{^{56}\mathrm{Fe}} \sim 930$ MeV for B around 2×10^{19} G.

We next consider stellar matter made out of quarks, electrons, and muons in β equilibrium, as possibly occurring in the interior of magnetars. It is worth mentioning that, in this case, the three different quarks bear different chemical potentials, determined by the chemical equilibrium conditions

$$\mu_d = \mu_s = \mu_u + \mu_e, \quad \mu_\mu = \mu_e.$$

We start by plotting the quark effective masses for different values of the magnetic field in Fig. 8. It is seen that the results for nonmagnetized matter ($B = 0$) almost coincide with the ones obtained for $B = 10^{18}$ G. A decrease of the s quark mass starts only at $\sim$0.8 fm^{-3}. This behavior has already been discussed in Ref. [20]. If the magnetic field is strong

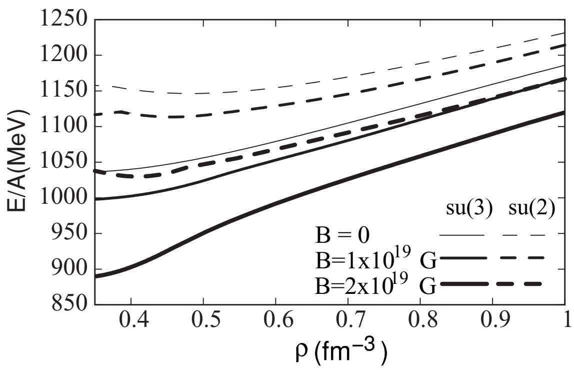

FIG. 7. Energy per nucleon as a function of density for $B = 0$, 10^{19}, and 2×10^{19} G within NJL su(2) and NJL su(3).

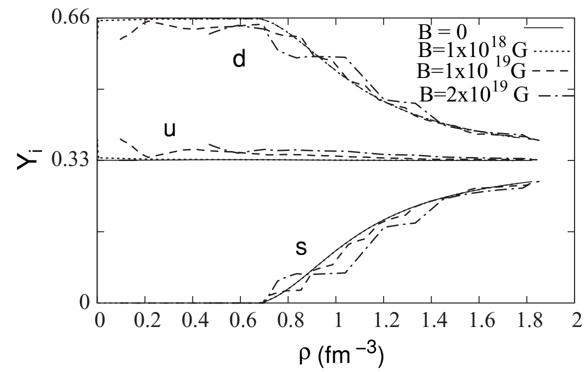

FIG. 9. Fraction of quarks in β-equilibrium quark matter for a constant magnetic field within NJL su(3).

enough the mass of quark s occurs in finite jumps that may give rise to an increase of the strangeness fraction as shown in Fig. 9.

The quark fractions $Y_i = \rho_i/\rho$, $i = u, d, s$, are shown in Fig. 9. Again the results for $B = 0$ are similar to the ones for $B = 10^{18}$ G. For strong enough fields the quark u fractions increase with a reduction of the quark d fraction. The quark s fraction has a sudden increase for $\rho \sim 0.7$ fm^{-3} but above $\rho \sim 0.9$ fm^{-3} remains below the $B = 0$ fraction.

In Fig. 10 the EOS for different values of the magnetic field is shown. For magnetic fields as large as $B = 10^{18}$G the differences are very small as compared with nonmagnetized matter. For larger fields there is an overall net softening of the EOS.

It is well known that at the surface the magnetic field should not be larger than $\sim 10^{15}$ G. We have introduced a density-dependent magnetic field as in Refs. [7,21]:

$$B_i = B^{\rm surf} + B_0 \left[1 - \exp\left\{ -\beta \left(\frac{\rho_b}{\rho_0} \right)^{\gamma} \right\} \right], \tag{26}$$

where $B^{\rm surf} = 10^{15}$ G is the magnetic field at the surface, B_i is the magnetic field at the interior of the star for large densities, and the parameters $\beta = 5 \times 10^{-5}$ and $\gamma = 3$ were chosen in such a way that the field increases fast with density to its central value but still describes correctly the surface of the star where the pressure is zero. We show the equations of state for quark matter in β equilibrium and a density-dependent magnetic field within both versions of the NJL model in Fig. 11. As implicit in Eq. (26), the field at the surface is 10^{15} G. The magnetic field makes the EOS harder with consequences in the gravitational and baryonic masses of compact stars, whose properties are obtained from the integration of the Tolman-Oppenheimer-Volkoff (TOV) equations, which use as input the EOS obtained with the density-dependent magnetic field. We are aware that the TOV equations were obtained for a system with spherical symmetry in hydrostatic equilibrium, and because the distribution of the magnetic field is not spherical, the TOV equations can only be used as an approximation in the present study. A correct integration of Einstein's equation was done in Ref. [22]. This, however, requires a large numerical effort that was not the aim of the present work. We should, therefore, take our conclusions on the star properties with care and interpret them as an average result.

The results obtained from the integration of the TOV equation are displayed both in Fig. 12 and in Table I, from where it is seen that both the gravitational and the baryonic masses increase with the increase of the magnetic field for an intensity larger than $\sim 5 \times 10^{18}$ G for the su(3) version and 10^{18} G for the su(2) NJL. However, the increase of the gravitational mass is larger than the increase of the baryonic mass because the contribution of the magnetic field becomes more and more important as the field increases. This explains the decrease

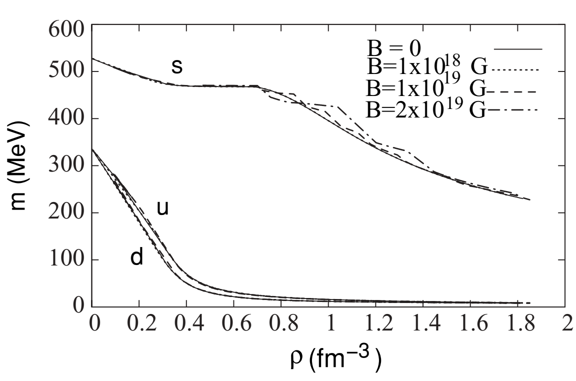

FIG. 8. The quark effective mass for β-equilibrium quark matter with a constant magnetic field within NJL su(3) as a function of the baryonic density.

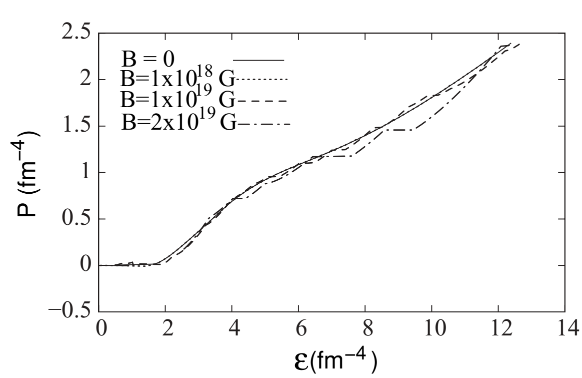

FIG. 10. Equation of state of β-equilibrium quark matter for constant magnetic fields within the NJL su(3).

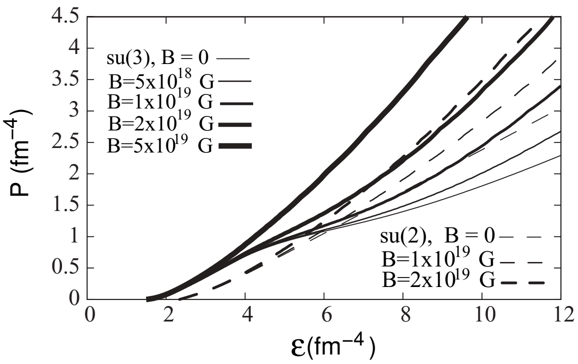

FIG. 11. Equation of state of β-equilibrium quark matter for a density-dependent magnetic field within NJL su(2) and NJL su(3). The EOS for $B = 0$ is also shown.

of the central energy/baryonic density for the stronger fields considered.

Another important effect of the field on the properties of the stars is the increase of the radius of the star with the largest radius, which may be as high as 9.5 km for the su(3) NJL. In general, the maximum mass star configurations for the su(2) version of the NJL model are smaller with smaller radius, ~7 km, in average 2 km smaller than the corresponding stars in the su(3) version of the NJL model.

Within the su(3) NJL the maximum mass configurations are always above $1.45M_\odot$ and may be as high as $1.86M_\odot$ for a central magnetic field of 5×10^{18} G. These numbers are within the masses of observed neutron stars. However, the su(2) version of the NJL model foresees too small star masses except for very large magnetic fields.

The effects of the anomalous magnetic moments has been shown to be relevant [23–25] and we intend to take them into account in the next calculations.

The color superconductivity (CS) [26], which allows the quarks near the Fermi surface to form Cooper pairs that condense and break the color gauge symmetry [27], is known to be present in the QCD phase diagram at sufficiently high densities. The effect of strong magnetic fields on the CS properties of quark matter, which can be drastic for sufficiently high fields, has already been studied by several authors [28]. It would be important to investigate how this CS phase could affect the properties of quark stars under strong magnetic fields. However, it could be that CS is only affected by magnetic fields stronger than the ones considered in the present article, which, however, predicts already a very high maximum mass, $M \sim 1.9M_\odot$. The largest magnetic field we got in the center of a quark star is 5×10^{18} G, while in Ref. [28] it is shown that a noticeable effect requires fields above $\sim 10^{19}$ G.

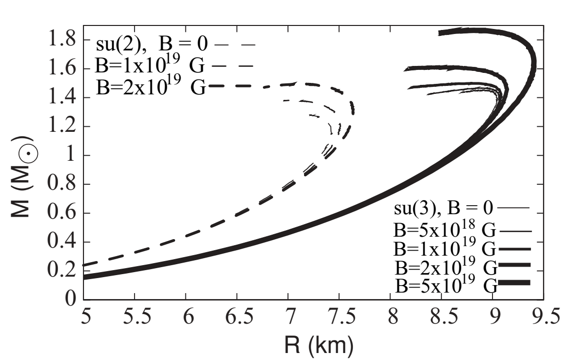

FIG. 12. Mass-radius curves for the families of stars within NJL su(2) and NJL su(3) corresponding to the EOS shown in Fig. 10. For $B \leqslant 10^{18}$, the curves coincide with the $B = 0$ results.

TABLE I. Maximum mass configurations for NJL su(3) and su(2), and several magnetic field intensities: the gravitational mass (M), baryonic mass (M_b), radius (R), central energy density (ϵ_c), baryonic density (ρ_c), and magnetic field (B_c) are given

B_0 (G)	M ($M_\odot$)	M_b ($M_\odot$)	R (km)	ϵ_c fm^{-4}	ρ_c fm^{-3}	B_c (G)
su(3)						
0	1.46	1.53	8.93	7.49	1.19	10^{15}
10^{18}	1.46	1.53	8.93	7.49	1.19	1.6×10^{17}
5×10^{18}	1.47	1.54	8.88	7.94	1.24	8.8×10^{17}
1×10^{19}	1.50	1.58	8.78	8.36	1.25	1.8×10^{18}
2×10^{19}	1.61	1.69	8.53	9.64	1.25	3.6×10^{18}
5×10^{19}	1.86	1.88	8.81	9.26	1.01	5.0×10^{18}
su(2)						
0	1.29	1.24	7.09	13.68	1.86	10^{15}
1×10^{18}	1.29	1.25	7.08	13.85	1.88	1.2×10^{17}
1×10^{19}	1.38	1.33	7.01	14.52	1.72	4.0×10^{18}
2×10^{19}	1.49	1.41	7.11	14.47	1.49	5.7×10^{18}

ACKNOWLEDGMENTS

This work was partially supported by the Capes/FCT No. 232/09 bilateral collaboration, by CNPq (Brazil), by FCT, by FEDER (Portugal) under Project CERN/FP/83505/2008, and by Compstar, an ESF Research Networking Programme.

APPENDIX: THE su(3) NJL MODEL IN THE MFA

In this appendix the main steps to obtain the NJL Lagrangian in the mean-field approximation are explicitly shown. First, we consider the $\mathcal{L}_{\rm sym}$ term given in Eq. (3). For later convenience, we define the matrix elements of Φ and its adjoint $\Phi^\dagger$ as [9]

$$\Phi_{ij} = \bar{\psi}_j(1-\gamma_5)\psi_i, \, \Phi^\dagger_{ij} = \bar{\psi}_j(1+\gamma_5)\psi_i,$$

where i and j are flavor labels. From these definitions, one can easily show that

$$\begin{aligned} \bar{\psi}_f(1-\gamma_5)\lambda_a\psi_f &= \mathrm{tr}(\lambda_a\Phi), \\ \bar{\psi}_f(1+\gamma_5)\lambda_a\psi_f &= \mathrm{tr}(\lambda_a\Phi^\dagger), \end{aligned} \tag{A1}$$

where tr is the trace operator in flavor space. So, adding and subtracting these expressions, we can rewrite the NJL symmetric four-point interaction term as

$$\begin{aligned} \mathcal{L}_{\rm sym} &= G\sum_{a=0}^{8}[(\bar{\psi}_f\lambda_a\psi_f)^2 + (\bar{\psi}_f i\gamma_5\lambda_a\psi_f)^2] \\ &= G\sum_{a=0}^{8}\mathrm{tr}(\lambda_a\Phi)\mathrm{tr}(\lambda_a\Phi^\dagger) = 2G\mathrm{tr}(\Phi\Phi^\dagger). \end{aligned} \tag{A2}$$

The summation involved in the latter equality can be performed noting that an arbitrary matrix A in the $N_f = 3$ flavor space, can be expanded in terms of Gell-Mann matrices as follows:

$$A = \sum_{a=0}^{8} c_a \lambda_a, \text{ with } c_a = \frac{1}{2}\mathrm{tr}(\lambda_a A). \tag{A3}$$

The expansion coefficients c_a are obtained using the Gell-Mann matrices' property: $\mathrm{tr}(\lambda_a \lambda_b) = 2\delta_{ab}$. So, we can write

$$\mathrm{tr}(AA^\dagger) = \mathrm{tr}\left(\sum_{a=0}^{8} c_a \lambda_a \sum_{b=0}^{8} c_b^\star \lambda_b^\dagger\right) = \frac{1}{2}\sum_{a=0}^{8}\mathrm{tr}(\lambda_a A)\mathrm{tr}(\lambda_a A^\dagger), \tag{A4}$$

where in the latter term we have used that the Gell-Mann matrices are hermitian, that is, $\lambda_a = \lambda_a^\dagger$. We then evaluate $\mathcal{L}_{\rm sym}$ in the mean-field approximation linearizing the interaction terms. We follow Refs. [9,10] approximating the product of two operators $\hat{O}_1$ and $\hat{O}_2$ by

$$\hat{O}_1\hat{O}_2 \approx \hat{O}_1\langle\hat{O}_2\rangle + \langle\hat{O}_1\rangle\hat{O}_2 - \langle\hat{O}_1\rangle\langle\hat{O}_2\rangle. \tag{A5}$$

Therefore, calculating explicitly the trace involved in Eq. (A2) and taking into account the aforementioned prescription, $\mathcal{L}_{\rm sym}$ can be written in the MFA as

$$\mathcal{L}_{\rm sym} = 4G\left[\phi_u u^\dagger u + \phi_d d^\dagger d + \phi_s s^\dagger s - \tfrac{1}{2}\left(\phi_u^2 + \phi_d^2 + \phi_s^2\right)\right], \tag{A6}$$

where we have used

$$\langle\bar{\psi}_i\psi_j\rangle = \delta_{ij}\phi_i \quad \text{and} \quad \langle\bar{\psi}_i\gamma_5\psi_j\rangle = 0. \tag{A7}$$

The only three nonvanishing terms are the condensates that were defined in Eq. (10). Finally, we consider the t'Hooft term, Eq. (4), which is a six-point interaction in the su(3) flavor space. Notice that term involves the product of three operators that we linearize analogously to Eq. (A5):

$$\hat{O}_1\hat{O}_2\hat{O}_3 \approx \hat{O}_1\langle\hat{O}_2\rangle\langle\hat{O}_3\rangle + \langle\hat{O}_1\rangle\hat{O}_2\langle\hat{O}_3\rangle + \langle\hat{O}_1\rangle\langle\hat{O}_2\rangle\hat{O}_3 \\ -2\langle\hat{O}_1\rangle\langle\hat{O}_2\rangle\langle\hat{O}_3\rangle.$$

So, in the MFA the determinants that appear in the t'Hooft term can be written as

$$\begin{aligned}
&\det{}_f(\bar{\psi}_f\mathcal{O}\psi_f) \\
&= \sum_{i,j,k}\epsilon_{ijk}(\bar{u}\mathcal{O}\psi_i)(\bar{d}\mathcal{O}\psi_j)(\bar{s}\mathcal{O}\psi_k) \\
&\approx \sum_{i,j,k}\epsilon_{ijk}[(\bar{u}\mathcal{O}\psi_i)\langle\bar{d}\mathcal{O}\psi_j\rangle\langle\bar{s}\mathcal{O}\psi_k\rangle + \langle\bar{u}\mathcal{O}\psi_i\rangle(\bar{d}\mathcal{O}\psi_j)\langle\bar{s}\mathcal{O}\psi_k\rangle \\
&\quad + \langle\bar{u}\mathcal{O}\psi_i\rangle\langle\bar{d}\mathcal{O}\psi_j\rangle(\bar{s}\mathcal{O}\psi_k) - 2\langle\bar{u}\mathcal{O}\psi_i\rangle\langle\bar{d}\mathcal{O}\psi_j\rangle\langle\bar{s}\mathcal{O}\psi_k\rangle.
\end{aligned}$$

Now, inserting the operator $\mathcal{O} = 1 \pm \gamma_5$ and using the properties given in Eq. (A7), we obtain the t'Hooft term in the MFA:

$$\mathcal{L}_{\rm det} = -2K(\phi_d\phi_s\bar{u}u + \phi_u\phi_s\bar{d}d + \phi_u\phi_d\bar{s}s - 2\phi_u\phi_d\phi_s). \tag{A8}$$

From Eq. (2) and Eqs. (A6) and (A8), the su(3) NJL Lagrangian in the MFA is given by

$$\begin{aligned}
\mathcal{L}_f^{\rm MFA} &= \bar{\psi}_f(\gamma_\mu(i\partial^\mu - q_f A^\mu) - \hat{M})\psi_f \\
&\quad - 2G\left(\phi_u^2 + \phi_d^2 + \phi_s^2\right) + 4K\phi_u\phi_d\phi_s,
\end{aligned}$$

where $\hat{M}$ is a diagonal matrix with elements defined in Eq. (11).

[1] I. V. Selyuzhenkov (STAR Collaboration), Rom. Rep. Phys. **58**, 049 (2006); D. E. Kharzeev, Phys. Lett. **B633**, 260 (2006); D. E. Kharzeev, L. D. MacLerran, and H. J. Waringa, Nucl. Phys. **A803**, 227 (2008).

[2] R. C. Duncan and C. Thompson, Astrophys. J. **392**, L9 (1992).

[3] C. Kouveliotou *et al.*, Nature (London) **393**, 235 (1998).

[4] D. P. Menezes, C. Providência, and D. B. Melrose, J. Phys. G: Nucl. Part. Phys. **32**, 1081 (2006); R. X. Xu, *Strange Quark Stars—A. Review*, in High Energy Processes, Phenomena in Astrophysics, Proceedings of IAU Symposium No. 214, edited by X. D. Li, Z. R. Wang, and V. Trimble, pp. 191–198; V. V. Usov, Phys. Rev. Lett. **80**, 230 (1998); Astrophys. J. **550**, L179 (2001); A. G. Aksenov, M. Milgrom, and V. V. Usov, Astrophys. J. **609**, 363 (2004); D. B. Melrose, R. Fock, and D. P. Menezes, Mon. Not. R. Astron. Soc. **371**, 204 (2006).

[5] N. Itoh, Prog. Theor. Phys. **44**, 291 (1970); A. R. Bodmer, Phys. Rev. D **4**, 1601 (1971); E. Witten, Phys. Rev. D **30**, 272 (1984); C. Alcock, E. Farhi, and A. Olinto, Astrophys. J. **310**, 261 (1986).

[6] Y. Nambu and G. Jona-Lasinio, Phys. Rev. **122**, 345 (1961); **124**, 246 (1961).

[7] D. P. Menezes, M. B. Pinto, S. S. Avancini, A. P. Martínez, and C. Providência, Phys. Rev. C **79**, 035807 (2009).

[8] T. Hatsuda and T. Kunihiro, Phys. Lett. **B198**, 126 (1987); V. Bernard, R. L. Jaffe, and U.-G. Meiner, Nucl. Phys. **B308**, 753 (1988); M. Takizawa, K. Tsushima, Y. Kohyama, and K. Kubodera, Nucl. Phys. **A507**, 611 (1990); S. Klimt, M. Lutz, U. Vogl, and W. Weise, Nucl. Phys. **A516**, 429 (1990); S. P. Klevansky, Rev. Mod. Phys. **64**, 649 (1992); P. Rehberg, S. P. Klevansky, and J. Hufner, Phys. Rev. C **53**, 410 (1996).

[9] T. Hatsuda and T. Kunihiro, Phys. Rep. **247**, 221 (1994).

[10] M. Buballa, Phys. Rep. **407**, 205 (2005).

[11] M. Buballa, Nucl. Phys. **A611**, 393 (1996).

[12] M. Buballa and M. Oertel, Phys. Lett. **B457**, 261 (1999).

[13] E. S. Fraga and A. J. Mizher, Phys. Rev. D **78**, 025016 (2008).

[14] http://mathworld.wolfram.com/HurwitzZetaFunction.html.

[15] B. Jancovici, Phys. Rev. **187**, 2275 (1969).

[16] R. C. Duncan, AIP Conf. Proc. **526**, 830 (2000).

[17] A. V. Kuznetsov, N. V. Mikheev, and M. V. Osipov, Mod. Phys. Lett. A **17**, 231 (2002); A. V. Kuznetsov and N. V. Mikheev, Phys. Rev. Lett. **89**, 011601 (2002).

[18] K. Schertler, S. Leupold, and J. Schaffner-Bielich, Phys. Rev. C **60**, 025801 (1999).

[19] D. Ebert, K. G. Klimenko, M. A. Vdovichenko, and A. S. Vshivtsev, Phys. Rev. D **61**, 025005 (1999); D. Ebert and K. G. Klimenko, Nucl. Phys. **A728**, 203 (2003); S. Chakrabarty, S. Mandal, and S. Chakrabarty, Phys. Rev. C **75**, 015805 (2007).

[20] D. P. Menezes and C. Providência, Phys. Rev. C **70**, 058801 (2004).

[21] D. Bandyopadhyay, S. Chakrabarty, and S. Pal, Phys. Rev. Lett. **79**, 2176 (1997).

[22] M. Bocquet, S. Bonazzola, E. Gourgoulhon, and J. Novak, Astron. Astrophys. **301**, 757 (1995); C. Y. Cardall, M. Prakash, and J. M. Lattimer, Astrophys. J. **554**, 322 (2001).

[23] A. Broderick, M. Prakash, and J. M. Lattimer, Astrophys. J. **537**, 351 (2000); A. Broderick, M. Prakash, and J. M. Lattimer, Phys. Lett. **B531**, 167 (2002).

[24] F. X. Wei, G. J. Mao, C. M. Ko, L. S. Kisslinger, H. Stocker, and W. Greiner, J. Phys. G **32**, 47 (2006).

[25] R. G. Felipe, A. P. Martinez, H. P. Rojas, and M. Orsaria, Phys. Rev. C **77**, 015807 (2008).

[26] M. G. Alford, K. Rajagopal, and F. Wilczek, Phys. Lett. **B422**, 247 (1998); R. Rapp, T. Schäfer, E. V. Shuryak, and M. Velkovsky, Phys. Rev. Lett. **81**, 53 (1998); I. Shovkovy, M. Hanauske, and M. Huang, Phys. Rev. D **67**, 103004 (2003); D. T. Son and M. A. Stephanov, *ibid.* **61**, 074012 (2000); **62**, 059902(E) (2000); M. Alford and S. Reddy, *ibid.* **67**, 074024 (2003).

[27] M. G. Alford, Annu. Rev. Nucl. Part. Sci. **51**, 131 (2001).

[28] K. Iida and G. Baym, Phys. Rev. D **66**, 014015 (2002); E. J. Ferrer, V. de la Incera, and C. Manuel, Phys. Rev. Lett. **95**, 152002 (2005); E. J. Ferrer, V. de la Incera, and C. Manuel, Nucl. Phys. **B747**, 88 (2006); E. J. Ferrer and V. de la Incera, Phys. Rev. Lett. **97**, 122301 (2006); J. L. Noronha and I. A. Shovkovy, Phys. Rev. D **76**, 105030 (2007); K. Fukushima and H. J. Warringa, Phys. Rev. Lett. **100**, 032007 (2008).